

Complex study on photoluminescence properties of YAG:Ce,Gd phosphors

V M Lisitsyn¹, Yangyang Ju¹, S A Stepanov¹ and N M Soschin²

¹ National Research Tomsk Polytechnic University, 30 Lenin Ave., Tomsk, 634050, Russia

²Scientific-Research Institute "Sycamore", Fryazino, 141195, Russia

E-mail: 1374586947@qq.com

Abstract: Luminescence characteristics of gadolinium co-doped yttrium aluminium garnet doped with cerium phosphors were studied. In this work, powder X-ray diffraction (XRD) spectra, elemental composition analyses, excitation and emission spectra, conversion efficiency of emission phosphor, corresponding (CIE) chromaticity colour coordinates and pulsed photoluminescence decay kinetic curves were investigated, all the measurements were performed at room temperature. The properties of the phosphors were studied by comparing the composition of the phosphors and their luminescent properties.

1. Introduction

Yellow colour phosphors based on yttrium aluminum garnet (YAG, $\text{Y}_3\text{Al}_5\text{O}_{12}$) are promising materials because of their good chemical and physical properties: excellent chemical stability at elevated temperature and under radiation stimulation, good emission characteristics under excitation. YAG phosphor is used to convert electrons to visible light in displays [1-5]. Ce^{3+} -activated phosphor $\text{Y}_{3-x}\text{Al}_5\text{O}_{12}:x\text{Ce}^{3+}$ (YAG:Ce) as a well-known efficient phosphor material is used to convert ultraviolet and blue LED radiation into yellow emission. It is assumed that the excitation of Ce^{3+} ion causes maximum absorbance in the blue region resulting in converting InGaN based blue LED radiation into a very broad intense yellow emission band and then combining the yellow emission with the non-absorbed blue emission from the blue LED to generate white light. However, it shows a low color rendering index (CRI). Thus in order to improve the quality of white light YAG:Ce can be doped with other rare earth ions, such as Gd^{3+} and Tb^{3+} [6]. Gd^{3+} (Gd^{3+} i.r. = 0.938 Å) has been added to substitute at the Y^{3+} (0.9 Å) site, which attributes to lattice distortion in the region of Ce^{3+} and shift of the emission band to a longer wavelength.

In the present study, industrial YAG phosphors with different concentration of Gd^{3+} were investigated.

2. Experimental details

Industrial YAG phosphors of SDL4000, SDL2700 and SDL3500 with different ratio of elemental composition were used for the present research. Information on the test samples is shown in Table 1. The elemental composition analyses of the samples were performed by a x-ray photoelectron spectroscopy (XPS) ESCALAB 250 with a PHI 5000Versaprobe-Scanning ESC Amicroprobe. The measurements were carried out by a monochromatic Al K α X-Ray source (500 μm , 60 W, 10 kV) with photon energy of 1486.6 eV. Survey scans (binding energies ranging from 0 to 1400 eV) were



performed using a 1 eV/step, while for higher resolution spectra of the Gd 4d, Ce 3d, O 1s, Al 2p, C 1s, and Y 2d peaks, the hemispherical analyzer pass energy was maintained with 0.05 eV/step.

The phosphors of SDL2700 and SDL3500 contain Gd and Ce except for Y, Al and O. Gd and Ce in phosphor SDL4000 were not detected because of its small content. We emphasize that the used method allows us to determine the composition of the sample on its surface.

The crystal structure of the measured phosphors was identified by using the powder X-ray diffraction (XRD) Rigaku smart lab with Cu, K α radiation generated at 40 kv/30 mA. The recorded XRD spectra were covered from 10° to 60° with increments of 0.02°.

The photoluminescence spectra of the samples were recorded by FLS980 spectrometer (Edinburgh instruments) with a xenon lamp (250–1000 nm) as an excitation source. CIE color coordinates in the yellow light region were determined by luminescence spectra of the investigated phosphors.

Table 1. Elemental composition of phosphors

No.	phosphor	Y	Al	O	Gd	Ce
1	SDL2700	4.48	24.13	64.49	6.22	0.68
2	SDL3500	13.47	26.8	57.18	1.26	1.29
3	SDL4000 (1)	16.6	25.83	57.57		
4	SDL4000 (2)	16.31	23.94	59.75		

3. Experimental results

3.1. Crystal structure

Figure 1 shows the XRD patterns of tested phosphors. For comparison, a standard YAG phase (PDF 09-1316 for Y₃Al₅O₁₂) was also inserted.

From the inset in figure 1, the diffraction peaks are in line with that of the standard YAG phase. It is clear that no impurity phases were formed, which are possible due to the dopant Ce³⁺ and Gd³⁺ ions. It can be found that the diffraction peak of (420) moves to the lower angle side with the increase of Gd³⁺ content relative to the position in the crystal. It is assumed [7] that the shift of the peak (420) is caused by lattice distortion and substitution of ions Y³⁺ (0.92Å) by ions Gd³⁺ (0.938Å).

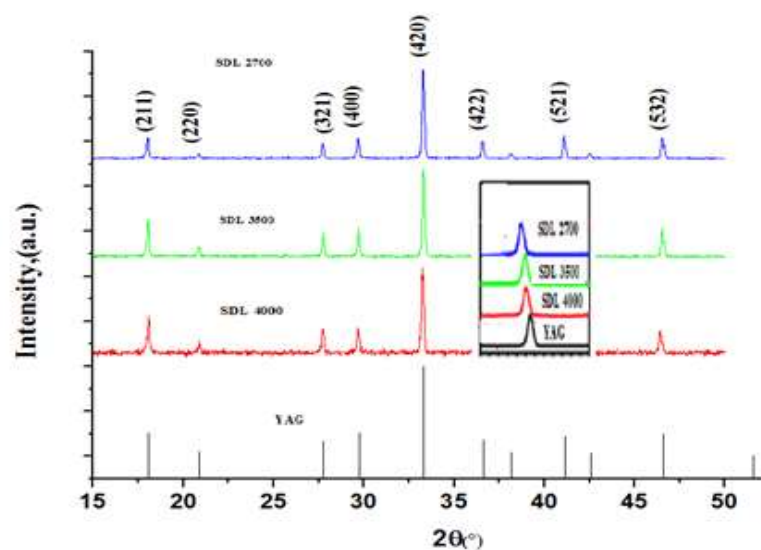


Figure 1. XRD patterns of SDL4000 (Y₃Al₅O₁₂), SDL3500 (Y_{2.6}Gd_{0.25}Al₅O₁₂:Ce_{0.15}), SDL2700 (Y_{1.24}Gd_{1.56}Al₅O₁₂:Ce_{0.2}) and standard Y₃Al₅O₁₂

3.2. Photoluminescence spectra and excitation spectra

Figure 2(a) shows excitation spectra of tested phosphors at the fixed emission wavelength of 560 nm, two bands can be seen in the region between 300 and 500 nm and these are peaked at 344 and 454 nm. The peak wavelength at 454 nm matches well with that of the light emitted by InGaN based blue LED; therefore, YAG phosphors can efficiently absorb blue light of the chip and convert it into a higher wavelength region.

Figure 2(b) (c) shows the photoluminescence (PL) emission spectra of YAG and YAG:Ce co-doped with Gd at a fixed excitation wavelength of 340 nm and 460 nm. The PL emission spectra show a broad emission band, which is supposed to be caused by Ce^{3+} ions with emission maxima occurring at 560 nm. It is known that Ce^{3+} is sensitive to the local crystalline field environment; therefore, lattice distortion by Gd ion substituting the Y^{3+} ion causes the shift in the emission band. It was observed from Figure 2 (b) and (c) that the substitution of Y ion results in red shift. However, the overall luminescence intensity decreases with the increase of Gd^{3+} .

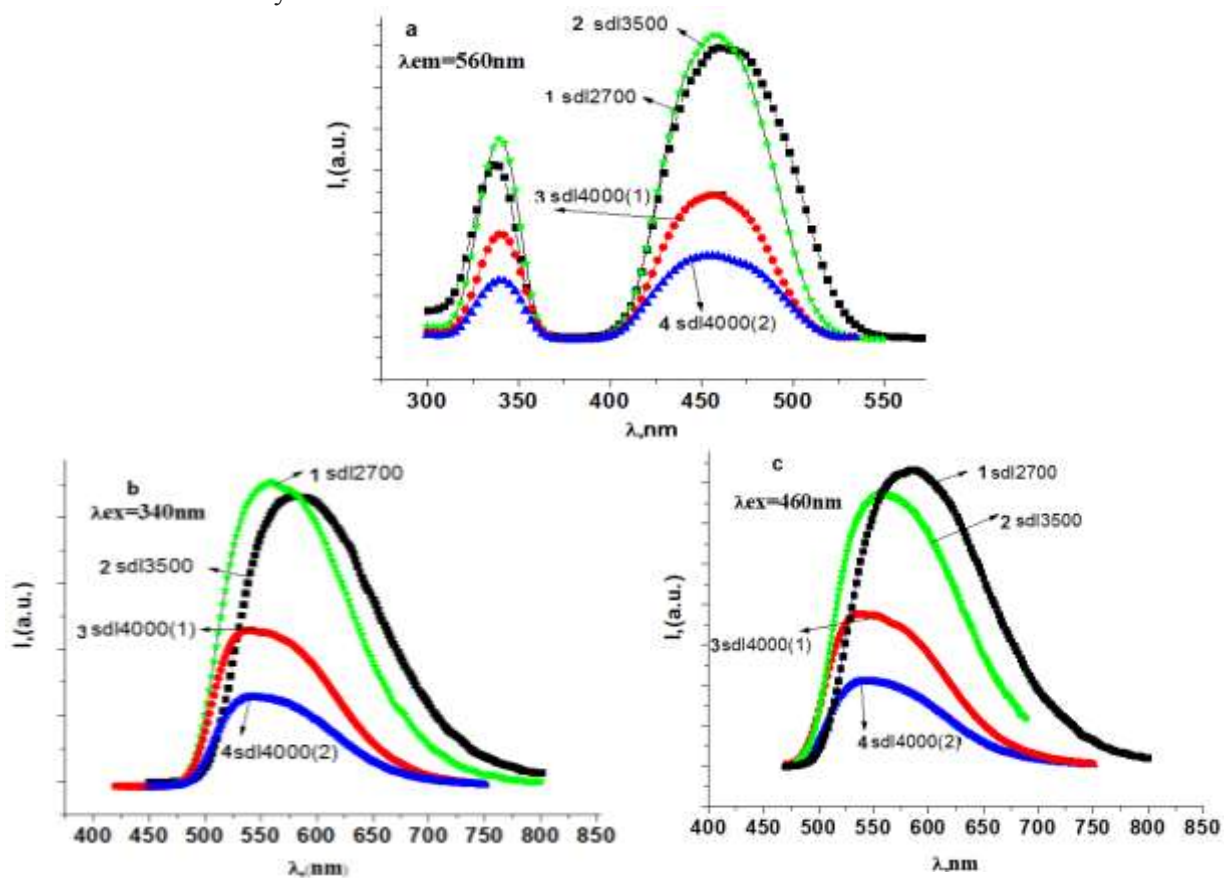


Figure 2. PL excitation spectra(a) and photoluminescent emission spectra (b, c) of phosphor samples SDL2700($\text{Y}_{1.24}\text{Gd}_{1.56}\text{Al}_5\text{O}_{12}:\text{Ce}_{0.2}$), SDL3500 ($\text{Y}_{2.6}\text{Gd}_{0.25}\text{Al}_5\text{O}_{12}:\text{Ce}_{0.15}$) and 2 SDL4000 ($\text{Y}_3\text{Al}_5\text{O}_{12}$)

The measurement results obtained for the spectral characteristics of the studied phosphors are summarized in Table 2. The positions of the luminescence bands do not depend on the area of the luminescence spectrum excited and the type of excitation. We can detect the following changes in the luminescence and excitation spectra.

The luminescence band of SDL4000 phosphor (~ 0.44 eV) under $\lambda_{\text{ex}} = 454$ nm is narrower than that of SDL2700 and SDL3500 (~ 0.485 eV) phosphors. The luminescence band of SDL4000 phosphor under $\lambda_{\text{ex}} = 344$ nm (~ 0.495 eV) is wider than $\lambda_{\text{ex}} = 454$ nm (~ 0.44 eV). The width of the

excitation band at 340 nm of all studied phosphors varies from 0.264 to 0.324 eV. The width of the excitation band at 460 nm of all studied phosphors varies from 0.390 to 0.450 eV.

Table 2. Measurement results obtained for the luminescence spectra and excitation of phosphors: peak value position and half band-width

phosphor	luminescence				excitation			
	$\lambda_{\text{ex}} = 460 \text{ nm}$		$\lambda_{\text{ex}} = 340 \text{ nm}$		In the region of 340nm		In the region of 460nm	
	$\Delta E, \text{ eV}$	$\lambda_{\text{max}}, \text{ nm}$	$\Delta E, \text{ eV}$	$\lambda_{\text{max}}, \text{ nm}$	$\Delta E, \text{ eV}$	$\lambda_{\text{max}}, \text{ nm}$	$\Delta E, \text{ eV}$	$\lambda_{\text{max}}, \text{ nm}$
SDL2700	0.487	584	0.489	582	0.264	336	0.450	459
SDL3500	0.484	560	0.487	558	0.294	339	0.390	459
SDL 4000(1)	0.435	539	0.486	540	0.313	339	0.396	456
SDL 4000(2)	0.447	541	0.504	542	0.324	339	0.426	456

3.3. Evaluation limiting values of light output at conversion of spectra in LED

The limiting values of the light output during spectrum conversion in phosphor were evaluated. The evaluation was carried out under the following conditions. We only take into account the energy losses in the process of converting chip radiation into luminescence in phosphor. In the spectrum of "white" light of LED is considered the proportion of "blue" radiation of chip that involved in the formation of the spectrum. The calculation method is described in [8], and the calculations were performed for two variants: the luminescence of phosphor is excited under $\lambda_{\text{ex}} = 344 \text{ nm}$ in the UV radiation region and in the blue radiation region under $\lambda_{\text{ex}} = 454 \text{ nm}$. In this work, it was assumed that the value of emission intensity at peak wavelength $\lambda = 454 \text{ nm}$ equals to the peak luminescence of phosphors at $\lambda_{\text{em}} = 560 \text{ nm}$ under $\lambda_{\text{ex}} = 454 \text{ nm}$. The results are presented in Table 3.

Table 3. Energy losses during spectrum conversion in phosphor and limiting values of light output

Phosphor	$\lambda_{\text{ex}} = 344 \text{ nm}$			$\lambda_{\text{ex}} = 454 \text{ nm}$		
	η_e	η_t	η_l	η_e	η_t	η_l
SDL2700	0.566	0.434	229	0.73	0.27	267
SDL3500	0.58	0.42	261	0.76	0.24	327
SDL4000(1)	0.593	0.407	277	0.76	0.24	349
SDL4000(2)	0.59	0.41	278	0.76	0.24	350

As follows from the calculated results, the values of energy losses in the process of converting chip radiation under $\lambda_{\text{ex}} = 344 \text{ nm}$ into luminescence of phosphor in the region of $\lambda_{\text{em}} = 560 \text{ nm}$ are not less than 44%, the luminous efficiency of the LED cannot be more than 280 lm/W. Accordingly, under $\lambda_{\text{ex}} = 454 \text{ nm}$, the values of energy losses are more than 27%, the luminous efficiency of the LED cannot be more than 350 lm / W.

3.4. CIE colour coordinates

Table 4 shows the chromaticity coordinate of phosphor emission. With the increase in the content of Gd^{3+} emission spectrum is approaching the ideal range of white light with $x = 0.33$ and $y = 0.33$.

Table 4. CIE colour coordinates of each tested phosphors

Phosphors	CIE color coordinates	
	x	y
SDL2700($\text{Y}_{1.24}\text{Gd}_{1.56}\text{Al}_5\text{O}_{12}:\text{Ce}_{0.2}$)	0.34	0.49
SDL3500($\text{Y}_{2.6}\text{Gd}_{0.25}\text{Al}_5\text{O}_{12}:\text{Ce}_{0.15}$)	0.45	0.53
SDL4000 (1)($\text{Y}_3\text{Al}_5\text{O}_{12}$)	0.42	0.55
SDL4000(2) ($\text{Y}_3\text{Al}_5\text{O}_{12}$)	0.43	0.55

3.5. The light output of LED with phosphors

The integrated spectral efficiency was measured by using an integrating sphere and calibrated spectrophotometer AvaSpec-ULS3648. The energy output η is the radiation flux ratio of phosphor to absorb the excitation flux. Two types of chips were used for excitation, which generate radiation with a stream of $173 \mu\text{W}/\text{cm}^2$ in the band with a maximum at 460 nm and $16\,730 \mu\text{W}/\text{cm}^2$ at 447 nm. Power of LED are almost 100 times different.

Table 5. The radiation energy efficiency of converting the phosphor emission into a blue band of the spectrum.

Phosphor	Radiation energy output η	
	$\lambda_{\text{ex}} = 460 \text{ nm}$	$\lambda_{\text{ex}} = 447 \text{ nm}$
SDL2700	0.422	0.331
SDL3500	0.438	0.359
SDL4000(1)	0.377	0.373
SDL4000(2)	0.404	0.394

As follows from the results, radiation energy output η almost independent on the power of the exciting radiation during the conversion process of SDL4000 phosphor. The change does not exceed 2.5%. However, the energy output of SDL2700 phosphor by 22% and in the SDL3500 phosphor by 18% is reduced, with increase power of LED in 100 times. This difference in energy output can be attributed to the fact that phosphors are sensitive to temperature variation.

4. Conclusions

Complex research on a group of phosphors based on YAG with different content of Ce^{3+} activator and co-activator Gd^{3+} was conducted. These impurities are intentionally not introduced to the SDL4000 phosphor, in which Ce^{3+} and Gd^{3+} were not detected by using XPS method. All the studied phosphors have a crystal structure in accordance with a typical body centered cubic structure of YAG ($\text{Y}_3\text{Al}_5\text{O}_{12}$); however, lattice distortion causes the shift of the peak (420). It is assumed that the lattice distortion is caused by substitution of ions Y^{3+} (0.92Å) by ions Gd^{3+} (0.938Å). This explanation is well correlated with the measurement results obtained for XRD patterns of the studied phosphors. However, the peak shift in the SDL4000 phosphor relative to the peak in the crystal is evidently due to the other factors. Perhaps crystal lattice distorted in the SDL4000 phosphor is formed in the synthesis of intrinsic defects lattice.

Upon excitation in the region of 344 nm and 454 nm, the position of luminescence bands of all investigated phosphors respectively at 580 nm of SDL2700, 560 nm of SDL3500 and 540 nm of SDL4000 phosphor. With the increase of Gd^{3+} content, the emission wavelength shows a great red shift, which is due to the crystal lattice distortion formed in the region of the luminous center. It is assumed that the emission center of phosphors is Ce^{3+} ion. Apparently, luminous center of the SDL4000 phosphor has the same nature, though Ce^{3+} is not intentionally introduced during synthesis. It is interesting to observe that the luminescence band of SDL4000 phosphor under $\lambda_{\text{ex}} = 344 \text{ nm}$ is broader as compared to that under $\lambda_{\text{ex}} = 454 \text{ nm}$.

This difference can be explained either by the presence of two different crystal structures of luminous centers, or one type of luminous centers with different environments. One of the centers is dominant in SDL2700, 3500 phosphors.

It can be considered that the luminescence characteristics depend not only on the composition of the doping activators and co-activators, but also on the presence of high concentrations of native defects in the crystal which were included during synthesis. It is difficult to ensure compliance with stoichiometry during formation of the crystal with a complex structure. Therefore, native defects are introduced in the crystal during synthesis. Native defects together with activators and co-activators can form complex defects which are called nanodefects [9].

Acknowledgments

This work was supported by the *Key Laboratory of Supramolecular Structure, Chemical Institute of Jilin University*. The authors are greatly indebted to Prof. Yue Wang at Jilin University. Thanks to doctoral student Yue Wei Zhang for his assistance in experimental work.

Reference

- [1] Jang H, BinIm W, Lee D, Jeon D and S Kim 2007 *J. Lumin.* **126** 371
- [2] Jung K and W Lee 2007 *J. Lumin.* **126** 469.
- [3] Zhou S, Fu Z, Zhang J and S Zhang 2006 *J. Lumin.* **118** 179.
- [4] Zhou Y, Lin J, Yu M, Wang S and Zhang H 2002 *Mater. Lett.* **56** 628
- [5] Blasse G and A Bril 1967 *Appl. Phys. Lett.* **11** 53
- [6] Jun Wang, Tao Han, Tianchun Lang, Mingjing Tu and Lingling Penga 2015 *Optical Engineering* **54** 117106
- [7] Lisitsyn V, Lukash V, Stepanov S and Y Ju 2016 *AIP Conference Proceedings* **1698** 060008
- [8] Xu M, Zhang Z, Zhu J, Zhao J and X Chen 2014 *J. Phys. Chem. C.* **118** 27000
- [9] Lisitsyn V, Stepanov S, Valiev D, Vishnyakova E, Abdullin H, Marhabaeva A and A Tulegenova 2016 *IOP Conf. Series: Materials Science and Engineering* **110** 012051